LIMNOLOGY
and
OCEANOGRAPHY: METHODS

Limnol. Oceanogr.: Methods 12, 2014, 323–337

A continuous flow isotope ratio mass spectrometry method for high precision determination of dissolved gas ratios and isotopic composition

Chawalit N. Charoenpong,[1,2,3] Laura A. Bristow,[1,4] and Mark A. Altabet[1]*

[1]School for Marine Science and Technology, University of Massachusetts Dartmouth, New Bedford, MA, USA
[2]Marine Chemistry and Geochemistry Department, Woods Hole Oceanographic Institution, Woods Hole, MA, USA
[3]Earth, Atmospheric and Planetary Sciences Department, Massachusetts Institute of Technology, Cambridge, MA, USA
[4]Nordic Center for Earth Evolution, Institute of Biology, University of Southern Denmark, Campusvej 55, 5230 Odense, Denmark

Abstract

Dissolved gas ratios and isotopic compositions provide essential information about the biological and physical mechanisms influencing N_2, O_2, and Ar in aquatic systems. Current methods available are either limited by overall cost, labor-intensive sample collection and analysis, or insufficient precision. Here, we present a new highly accurate and robust method for sample collection and subsequent simultaneous measurement of the dissolved gas ratios (N_2/Ar and O_2/Ar) and isotopic compositions ($\delta^{15}N_2$ and $\delta^{18}O_2$) in seawater. The relatively simple sampling procedure using low cost materials enables collection of hundreds to more than a thousand discrete samples on a single research cruise. Samples can be preserved and stored at room temperature and maintain their integrity for many months. Laboratory analysis employs an on-line extraction system coupled to a multi-collector isotope ratio mass spectrometer (IRMS). A continuous flow of He carrier gas completely degasses the sample, and passes through the preparation and purification system before entering the IRMS for analysis. The use of this continuous He carrier permits short analysis times (less than 8 min per sample) as compared with current high-precision methods. In addition to reference gases, calibration is achieved using air-equilibrated water standards of known temperature and salinity. Assessment of reference gas injections, air equilibrated standards, as well as samples collected in the field shows the accuracy and precision of this new method to be equal to or better than current standard techniques.

Dissolved gases are powerful tracers for physical and biogeochemical processes in aquatic systems. N_2, O_2, and Ar are typically the three most abundant dissolved gases in the ocean, and deviations from their saturation concentrations can be used to assess influencing biological and physical processes. O_2 has long been used to assess primary production and estimate carbon export in marine environments (e.g., Gaarder and Gran 1927; Quay et al. 2010). Numerous studies have examined the ratio of this nonconservative species to inert Ar to delineate the effects of biological from physical processes such as bubble injection and temperature changes (Emerson et al. 1999; Hamme and Emerson 2004). In low oxygen environments, N_2 is produced by microbially mediated N-loss processes (denitrification and anammox), and these relatively small biogenic additions are detected by high precision measurement of N_2/Ar (e.g., Kana et al. 1998; Devol et al. 2006; Chang et al. 2010, 2012). The isotopic compositions of these dissolved gases, provide further insight into biogeochemical processes and their partitioning. Use of the $\delta^{18}O$ of dissolved O_2 ($\delta^{18}O_2$) to assess production and respiration in the ocean goes back to Kroopnick and Craig (1976). Studies to date have used this parameter to partition the contributions of water column and benthic respiration, mixing, and gas exchange (Bender and Grande 1987; Quay et al. 1993; Quay et

*Corresponding author: E-mail: ccharoenpong@whoi.edu

Acknowledgment

We thank the BATS team for measuring physical parameters and dissolved oxygen on the cruise as well as Elizabeth Lee for her help during the sampling. Support on board was offered by the officers and crew of the R/V *Atlantic Explorer*. Also, we are indebted to Pia H. Moisander (PHM) who led the cruise at BATS and was the PI of the project that funded the field sampling. Ralph Keeling supplied us with the atmospheric air reference. Finally, we thank Jennifer Larkum, Santhiska Pather, and Annie Bourbonnais for their assistance in the lab. CNC was funded by Thailand's Ministry of Science and Technology Fellowship and University of Massachusetts Dartmouth research/teaching assistantship, and this work was funded by NSF OCE-0623199 to MAA, NSF OCE-0851092 to MAA, and NSF OCE-1130495 to PHM and MAA. We gratefully acknowledge Michael DeGrandpre and two anonymous reviewers for their constructive reviews of the manuscript.

DOI 10.4319/lom.2014.12.323

al. 2010). The $\delta^{15}N$ of dissolved N_2 ($\delta^{15}N_2$) has been used as a potent tracer for denitrification (e.g., Fuchsman et al. 2008).

Amongst many methods to measure dissolved gases in the ocean, the determination of their ratios by mass spectrometry has become standard as a powerful technique (Emerson et al. 1999). Several analytical approaches are commonly used at present; membrane inlet mass spectrometry (MIMS) (e.g., Tortell 2005; Kana et al. 1994) and equilibrator inlet mass spectrometry (EIMS) (e.g., Cassar et al. 2009), both use quadrupole mass spectrometers as detectors and are capable of high-frequency, at-sea measurements. High throughput of samples at relatively low cost allows for resolution of fine-scale temporal and spatial variations but the MIMS and EIMS approaches are compromised by relatively lower precisions: ±19‰, and ±7‰ for O_2/Ar and N_2/Ar, respectively (Tortell 2005). They are similarly unsuitable for natural abundance isotope measurements. By contrast, isotope ratio mass spectrometry (IRMS) can achieve very high precisions of 0.4‰ and 0.6‰ for O_2/Ar and N_2/Ar ratios (Emerson et al. 1991) on discrete samples in the laboratory. The latter technique can also provide the isotopic composition of the dissolved O_2 and N_2 at high precision (0.04‰ for $\delta^{18}O_2$ and 0.03‰ for $\delta^{15}N_2$: Emerson et al. 1991). Though the method described in Emerson et al. (1991) achieves very high precision and accuracy, it is unsuitable for real-time data sampling and its wide use for discrete samples has been limited by the expense of a difficult and time-consuming field sampling procedure and relative low analytical throughput in the laboratory.

Our major goals in developing a new approach for dissolved gas analysis was to dramatically lower costs and increase analytical throughput while maintaining or exceeding the precision and accuracy of the best current techniques for simultaneous N_2/Ar, O_2/Ar, $\delta^{15}N_2$ and $\delta^{18}O_2$ determination. Accordingly, we have developed a method that uses off-the-shelf sampling materials and on-line extraction procedures for high analytical throughput in the laboratory. Therefore, our benchmark for precision and accuracy is the method described in Emerson et al. (1991) and Quay et al. (1993)—further referred to as the "EQ benchmark" method.

Our analytical strategy centers around use of a multicollector isotope ratio mass spectrometer (MC-IRMS) to achieve the highest precision and most rapid analysis. Our instrument (GV IsoPrime) is fitted with collectors for the coincident acquisition of masses 28 ($^{14}N^{14}N$), 29 ($^{15}N^{14}N$), 32 ($^{16}O^{16}O$), 33 ($^{17}O^{16}O$), 34 ($^{18}O^{16}O$), and 40 (^{40}Ar) allowing for all the species of interest to be determined simultaneously. Whereas our approach is similar to the EQ benchmark in this respect, we differ in the use of a continuous He carrier to fully extract dissolved gases and transport them through an on-line preparation system to the mass spectrometer inlet. Both artificial gas mixtures and air-equilibrated water of known temperatures and salinities are used as calibration standards.

We have explored a number of sampling schemes and a variety of materials. In all cases, the intent was to allow for rapid filling and sealing of sample bottles without headspace and return to the laboratory without leakage or bubble formation. As the sample analysis method involves gas extraction of the whole water sample, lack of headspace, and bubbles is critical given the relatively low solubility of the gases of interest. Described below are the sampling materials and methods deemed optimal after numerous comparisons including tests designed to mimic the experience of samples collected remotely and returned to the laboratory for analysis. Sample lifetime of many months in the laboratory is also a practical requirement that we have evaluated.

Materials and procedures

Sampling materials

Sixty milliliters borosilicate glass serum bottles (Wheaton, product #223746) are used along with 20 mm butyl rubber stoppers (Microliter Analytical, product # 20-20025) and Al ring seals (Microliter Analytical, product # 20-0000AS). This bottle volume was found convenient for both sampling as well as providing more than sufficient material for analysis. The stoppers specified allow for sample expansion and pressurization with moderate warming and were sufficiently gas impermeable to permit storage for many months (see below). These materials are relatively inexpensive (c.a. $2/sample) especially compared with the custom built flasks used for the EQ benchmark method. In addition, these glass bottles can be easily cleaned and reused. We found that multiple rinses with deionized water and combustion (450°C for several hours) are sufficient for cleaning these bottles. The latter removes any organic matter which could cause bubbles to stick to the inner wall during sampling. A glass bead (Fisherbrand, product# 10-310-1) is placed in the 60-mL combusted bottle before combustion or sampling to promote mixing of preservative after sealing.

Optimized sample collection procedures

Sequential illustrations of the procedure are shown in Fig. 1. Our dissolved gas samples are collected as soon as possible after the water sample comes up to the surface before any other types of sampling except for other gaseous parameters such as Winkler oxygen. The serum bottle is placed in a plastic filling container, and water is gravity fed from a Niskin bottle or similar sampling device through natural rubber latex (Fisherbrand, product# 14-178-2C) or silicone (Fisherbrand, product# 14-176-332E) tubing. After the tubing is connected to the Niskin outflow, the water sample is allowed to flow slowly through, controlled by manual pinching. Before sample collection commences, the first 20 mL water (or more if needed) is discarded while the tubing is lightly tabbing throughout its length, dislodging any bubbles out of the tubing along with the discarded water. The tubing is then placed at the base of the serum bottle and the bottle is filled slowly, ensuring it is free of any bubbles. During the first few seconds of filling, the tubing should be moved up and down to prevent any bubbles attaching to the outside wall. After which,

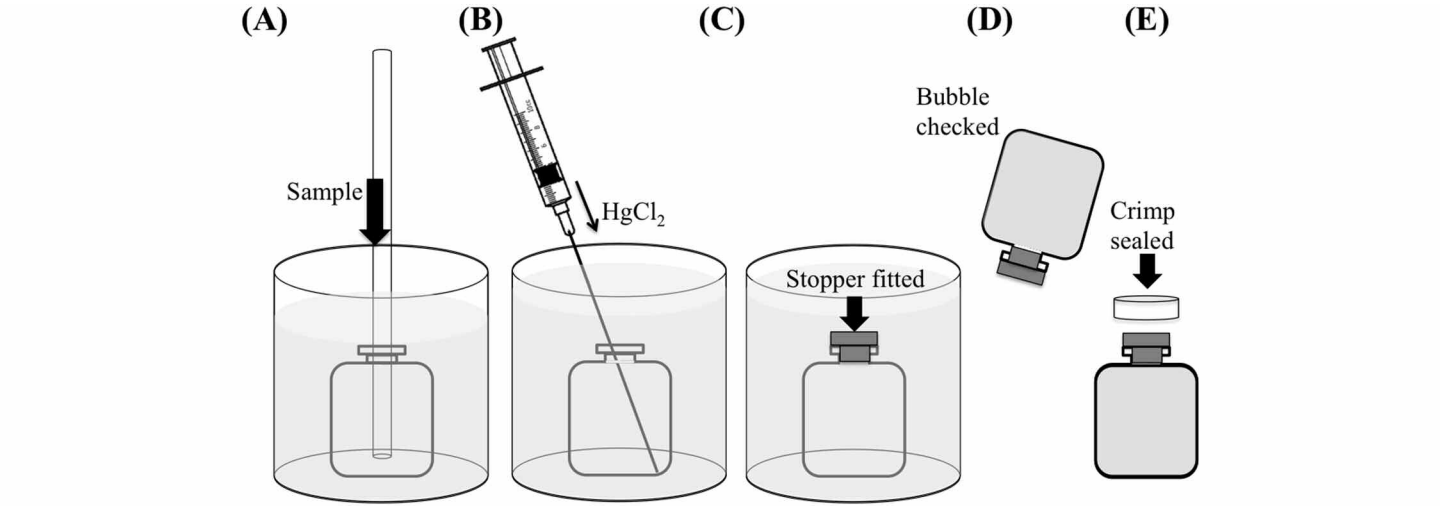

Fig. 1. Sampling protocol. (A) Bubble-free sample water from the Niskin bottle is fed into the bottom of the serum bottle. Water is allowed to overflow into the filling container until the bottle is completely submerged. (B) While totally submerged under water, $HgCl_2$ is added to the bottom of the bottle through a long blunt needle connected to a syringe. (C) The butyl stopper is fitted. (D) The bottle is turned upside down and gently tapped to check for bubbles. (E) Aluminum crimp is sealed over the stopper.

the end of the tube should be kept still at the bottom of the bottle to avoid splashing, which may result in bubble formation and/or oxygenation (especially for samples from a low oxygen setting). The water is allowed to overflow until the bottle is completely submerged. The plastic filling container should therefore be sufficiently large to permit water to cover the serum bottle's mouth as well as have sufficient room for manipulation of materials. The filling tube is then withdrawn making sure to slow the flow to a full stop as it clears the mouth of the serum bottle. While still submerged, 100 μL saturated $HgCl_2$ solution is added to the bottom of the serum bottle using a syringe with a 15-cm-long 18-gauge pointless needle. The butyl rubber stopper is inserted, making sure no small bubbles are sticking to its interior surface. The serum bottle is subsequently removed from the filling container, and carefully checked for bubbles. If no bubble is found, the bottle is immediately aluminum ring sealed, and then gently shaken to mix the preservative. The bottle needs to be discarded if even the smallest bubble is observed.

Samples are stored at room temperature until analysis. We have found that for typical ocean samples, warming to room temperature causes sufficient pressurization to prevent bubble formation even during air transport. These materials can tolerate warming from 4°C to 25°C though there is considerable bulging of the stopper. Nevertheless more extreme heating or cooling of samples should be avoided if possible. Before analysis, bottles are again checked for bubbles. Bubble formation can either be attributed to cavitation caused by contraction in sample volume or air seepage due to improper sealing (for this latter case, the samples should be discarded). One of the most common cavitation scenarios is when the sample water on collection is warmer than the temperature of storage. As cavitation bubbles are created from the contraction of liquid, once these void spaces are reabsorbed back to the liquid phase the gas composition in the sample is not altered. This can be accomplished by gently warming the bottles to c.a. 30°C to 35°C in a water bath before analysis.

Sample preparation system

A schematic of the preparation system is shown in Fig. 2. At the heart of this system lies the custom-made gas extractor, comprised of a 15-cm long glass tube fitted with gas-tight bottom and top. A continuous He flow (at 90 mL/min) passes through a fine frit (Ace Glass, product# 7176-103) at the base of the extractor and exits through a 1/16-inch OD stainless steel tubing (RESTEK, product# 21510) at the top. Identical tubing is used throughout the rest of the setup, unless noted otherwise. Meanwhile, the water sample from the serum-capped bottle is simultaneously pumped into and out of the extractor using a valveless metering pum*p* (Fluid Metering, product# QG400) at approximately 10 mL/min, whereas He gas is being concurrently introduced at 5 psi to prevent vacuum formation within the serum bottle. This metering pump model was selected because of its ability to maintain constant low flow and unique design involving only one moving part, which under our processing conditions eliminates the production of bubbles by cavitation. To avoid water from getting carried further downstream of the gas extractor in the He carrier, the water level in the gas extractor is carefully controlled by positioning the exit tube for the sample halfway between the base and top of the extractor setup (Fig. 2). In the extractor, the water sample is stripped of its dissolved gas content, which is carried further downstream by the He carrier gas into the gas purification part of the system. For frothy samples (such as those with high dissolved organic matter content), the foam

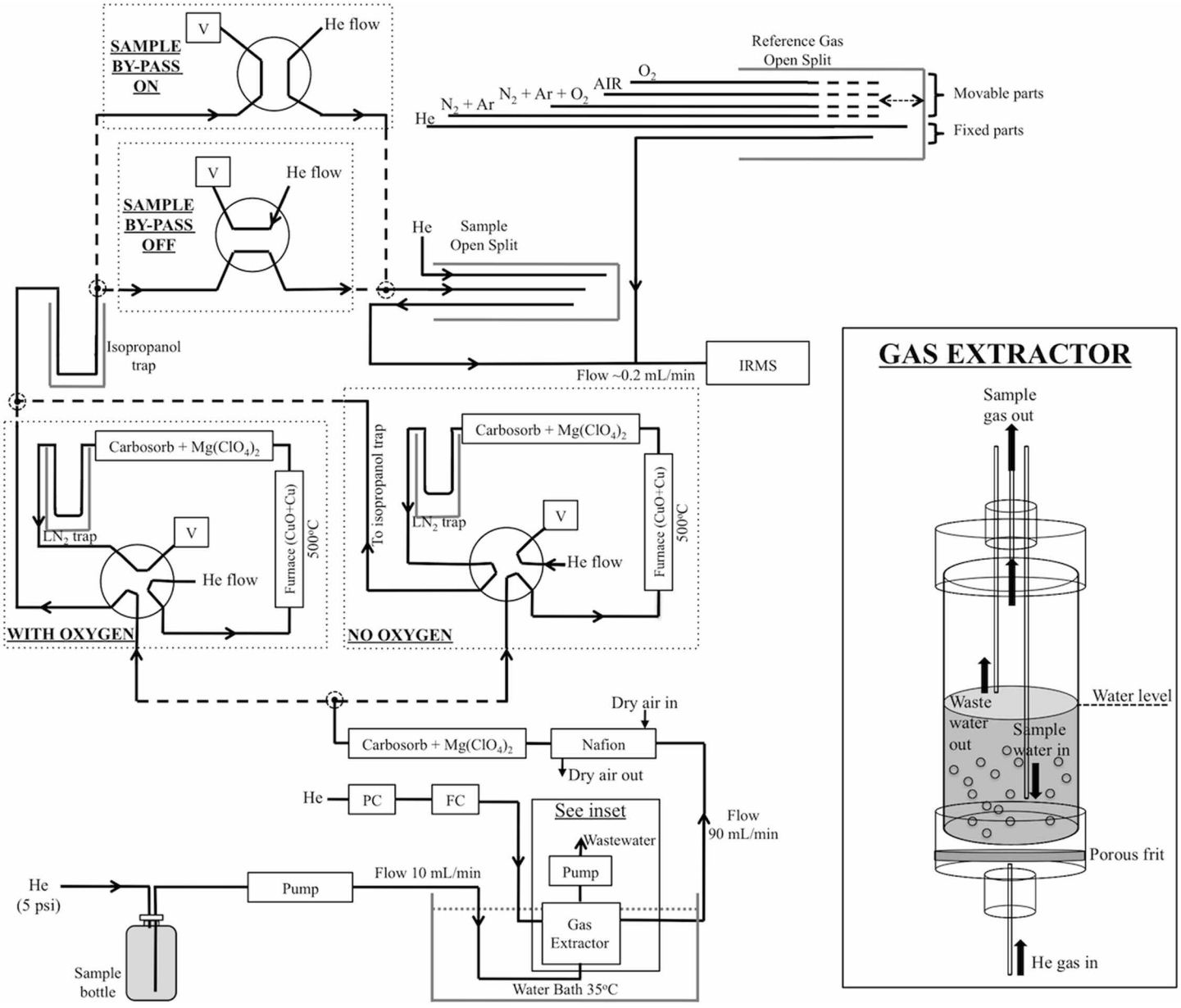

Fig. 2. Schematic diagram of the gas extraction and preparation system. PC: Pressure Controller, FC: Flow Controller, and V: Vent. The dotted boxes and lines show alternative routes for the gas flow, which is controlled by the switching of the Valco valves. The first set controls whether the sample gas will be passed through the reduction column to remove O_2 whereas the second set controls the sample gas bypass. Detail of the gas extractor is shown in the inset.

created through bubbling inside the gas extractor could introduce some water into the system downstream. To avoid this problem, intermittent flushing with deionized water between samples is recommended to reduce frothiness developed within the gas extractor. Quantitative gas extraction was a key requirement in the development of this technique. Our specified sample water and extraction He gas flows were chosen to meet this requirement as well as meet the needs for sufficient IRMS signal intensity for precise analysis, short system response times, and modest sample water consumption. Quantitative extraction was verified by changing sample water flow by ± 30% and observing both a linear relationship between flow rate and IRMS signal intensity for masses 28, 32, and 40 as well as invariant gas and isotopic ratios.

Gas flow after the extraction step goes through a Nafion drier (Perma Pure, product# MD-110-48S-2) to remove H_2O and then through a chemical trap filled with magnesium perchlorate and Carbosorb™ granules to remove any remaining H_2O and CO_2, respectively. Under software control the flow can be selected to undergo "with oxygen" or "no oxygen" mode

Table 1. Comparison of precisions reported in this study and those reported in the benchmark method (Emerson et al. 1991).

	N_2/Ar (‰)	O_2/N_2 (‰)	O_2/Ar (‰)	$\delta^{15}N_2$ (‰)	$\delta^{18}O_2$ (‰)
SD of standard gas replicates					
This study:					
Ref gas: N_2 + Ar + O_2 (n = 105)	0.22	0.23	0.28	0.02	0.04
Ref gas: N_2 + Ar (n = 100)	0.08	—	—	0.02	—
Emerson et al. (1991)	0.2	0.3	0.3	0.02	0.03
SD of water standards					
This study:					
Air-equilibrated SW stds (*n* = 43)	0.23	0.51	0.53	0.02	0.09
Average difference of pairs, same sample					
This study:					
BATS (Aug 12) (*n* = 24)	0.59	1.03	1.04	0.02	0.22
Emerson et al. (1991)	0.6	0.8	0.4	0.03	0.04

Note: For the two working reference gases and air-equilibrated seawater standards used in this study, numbers reported are the means of standard deviations of repeated measurements from a single analysis day. For the BATS samples, the values reported are the means of difference of pairs (randomly selected from the triplicate samples) from each depth. All numbers reported here are in ‰. For N_2/Ar, O_2/N_2, and O_2/Ar, the ratio SD or difference is converted to ‰ by dividing it by its average value and then multiplying the result by 1000‰.

through the six-port Valco valve (detail on mode switching is outlined in the subsequent section; *see* "Sample analytical procedure"). The former mode is used for measurements of O_2/Ar and $\delta^{18}O_2$ whereas the latter for N_2/Ar and $\delta^{15}N_2$. Removal of O_2 is essential for highly accurate measurements of both N_2/Ar and $\delta^{15}N_2$ due to interferences produced by variations in O_2/N_2 (see "Correction for varying O_2/N_2"). This is achieved through passing the sample gas over hot (450°C) CuO/Cu granules to convert any hydrocarbons or CO to CO_2 and to remove O_2. During this process, nitrogen oxides (including NO and N_2O) are also reduced to N_2. NO is usually found at pmol/kg concentrations (e.g., Ward and Zafiriou 1988) whereas N_2O is found in the nmol/kg range (e.g., Bange et al. 2001; Walter et al. 2006) in the open ocean. On the other hand, N_2 has an equilibrium concentration of 501 μmol/kg at t = 10°C and S = 35 (Hamme and Emerson 2004). Because both are NO and N_2O present at very low concentrations as compared with N_2, the contribution of N_2 produced from the reduction these two nitrogen oxides to the total N_2 gas passing through the reduction column is negligible and can be easily removed by adding a liquid N_2 trap upstream of the furnace. In addition, this subsystem includes a chemical trap filled with magnesium perchlorate and Carbosorb granules followed by a liquid nitrogen trap to remove any remaining H_2O or CO_2 produced. The "with oxygen" mode simply bypasses the shunt going into the reduction column.

Regardless of O_2 mode, an isopropanol trap (–50°C; Neslab CryoCool 60 immersion cooler) is used to remove any remaining trace contaminants before entering the 4-port Valco valve, which enables a sample by-pass mode during reference gas analysis. When the by-pass is off, sample gas flow is directed into the sample open split and in turn into the IRMS for analysis. When the by-pass is on, sample flow is instead vented to atmosphere and a make-up He flow enters the sample open split, and in turn, the MC-IRMS. For reference gas introduction, a custom built open-split system that permits mixing of gases is used with 2 stationary and 4 movable fused quartz capillaries. One of the stationary capillaries is for the He carrier and is positioned upstream to all others and the other is the outflow carrying the gas to the MC-IRMS. Movable capillaries are used for reference gas introduction. Their small internal diameter (50 μm) restricts flow sufficiently to achieve an appropriate range in IRMS signal intensity that is manually adjusted using Porter regulators to vary head pressure. We use the reference gases: 1) Air, 2) O_2, 3) N_2 + Ar + O_2, and 4) N_2 + Ar supplied from compressed gas tanks (Fig. 2). The latter two are artificial mixtures at near the ratios found in seawater. Through software control controlling 24V DC solenoids, which in turn, drive air pistons, each capillary can be inserted upstream of the outflow capillary allowing the gas to be carried into the outflow tube to the MC-IRMS. The He flow into the two open splits, 50 to 90 mL/min, is much greater than the flow into the MC-IRMS. Manually adjusting the flow of each reference gas also easily creates a desired gas mixture, when two or more reference gas capillaries are inserted allowing efficient calibration for the influence of variable O_2/N_2.

References and standards

Two reference gases are used in our method: N_2+Ar+O_2 for the "with O_2 mode" and N_2+Ar for the "no O_2 mode." They are made up by a local commercial gas supplier such that their gas ratios are within the typical ranges found in seawater. Both are tested for reproducibility by repeated injections at the beginning of each day (typical precisions are shown in Table 1). For air-equilibrated water standards, 1-L glass bottles filled with filtered seawater (using Whatman GF/F glass fiber filter with 0.7 μm nominal pore size) are kept at specified temperature by

high precision water baths (± 0.1°C). They are constantly stirred with an overhead mixer for at least 12 hours before use to allow full equilibration. In addition, salinity is checked immediately before analysis as it can affect the gas solubilities. Before sample analysis, typically two standards at a high and low temperature are tested and closeness to expected values as well as their reproducibility are used to assess system performance (precisions shown in Table 1). Usually, there are small offsets from expected values, which are used to correct sample results. Water standards are also run periodically throughout a day-long analytical run to assess stability (allowing a drift correction to be applied if necessary) and account for the day-to-day variations causing the abovementioned offsets.

Sample analytical procedure

The analysis of a single sample takes less than 8 minutes and consumes approximately 50 mL water sample. At the beginning of each run, a long needle connected to the pump intake is inserted to near the bottom of the serum bottle along with a short pressurization needle connected to the autosampler unit (GC PAL by LEAP Technology). An automated software procedure is used to control the flow of sample and reference gas into the system. In a typical run (see Fig. 3), the baseline is measured during the first 30 s after which the N_2+Ar+O_2 reference gas is injected followed by the gas mixture of N_2+Ar and O_2 at a low signal intensity while the sample by-pass is on. During this interval with the by-pass on, sample

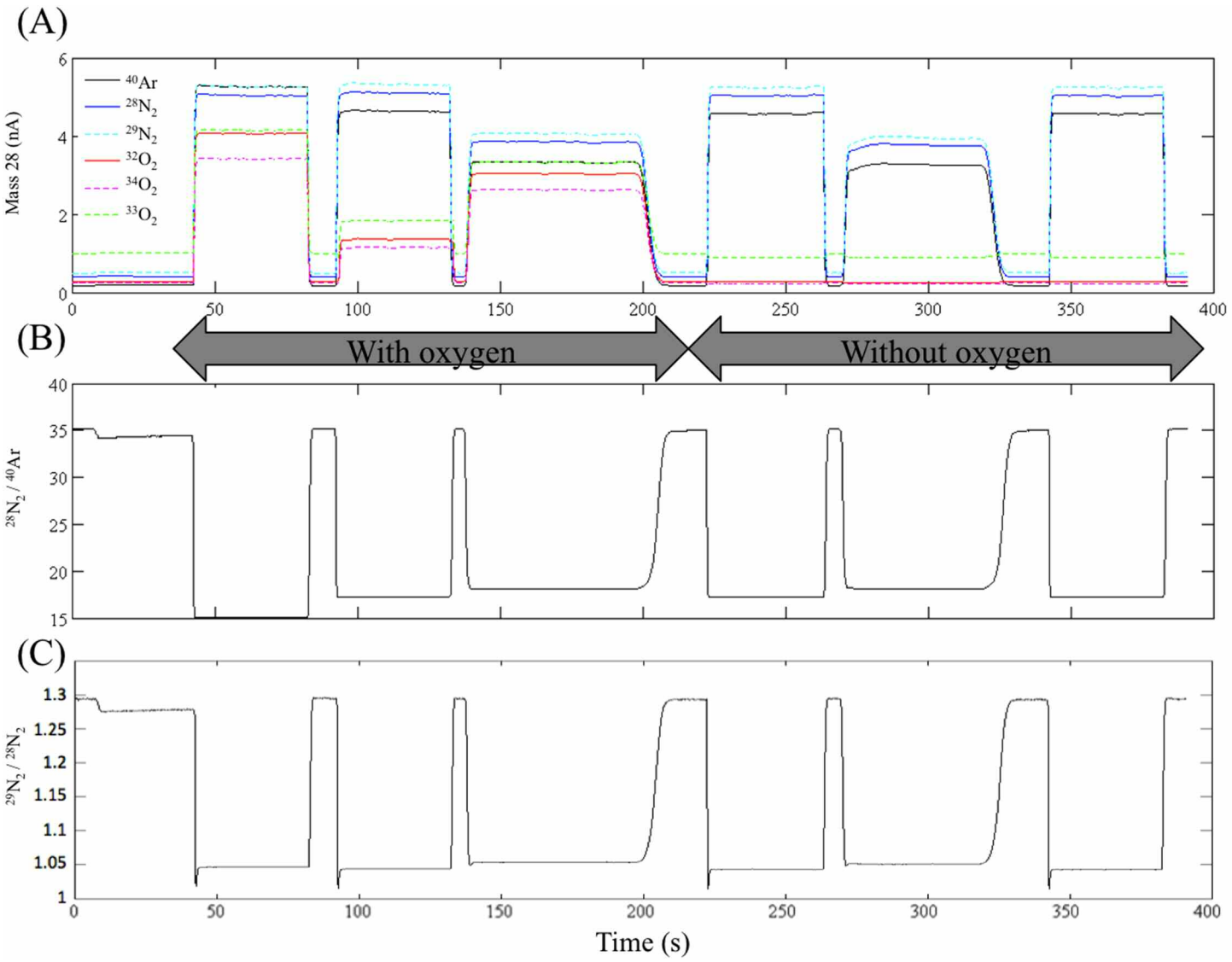

Fig. 3. Typical chromatogram (A) showing sequence of reference gas (Ref) and sample gas (Sam) injections. Peak 1 (Ref): N_2 + Ar + O_2, Peak 2 (Ref): N_2 + Ar and low O_2 mix, Peak 3 (Sam): without O_2 removal, Peak 4 (Ref): N_2 + Ar, Peak 5 (Sam): with O_2 removal, Peak 6 (Ref): N_2 + Ar. Each mass (assigned with a different color) has its own scale. Shown in the chromatogram above is the scale for the major mass, 28, in nanoamp (nA). (B) $^{28}N_2/^{40}Ar$ and (C) $^{29}N_2/^{28}N_2$ ratios are plotted throughout the analysis.

water is pumped into the gas extractor to stabilize at constant sample signal intensities before analysis and continues till the end of the sample analysis. The sample by-pass is then turned off to allow the sample gas to enter the IRMS. Then, the by-pass is turned back on allowing the sample gas flow to be directed to the O_2 removal furnace while the first N_2+Ar reference gas pulse is introduced. After turning the sample by-pass, the oxygen free sample gas peak follows. Finally, the sample by-pass is turned on again and the second N_2+Ar reference gas peak is injected. All injections of the reference gases and sample gases are controlled by the software-programmed valves, and their sequence and timing has been designed to produce well separated, flat-top peaks as seen in a typical chromatogram (Fig. 3). All reference gases are injected for 45 s while the sample gases are injected for 70 s. The longer time required for the sample peaks was found necessary for sufficient data integration and optimal precision. Individual chromatograms are checked for the flatness of the peak's top and stability of gas ratios to ensure the accuracy of measurements.

The gas ratios and isotopic compositions of the sample gas are calculated by the IonVantage software, which we program to report observed gas ratios (R) and delta values of the sample against the reference gas (standard):

$$\delta = \left(\frac{R_{sample}}{R_{standard}} - 1 \right) \times 1000 \quad (1)$$

Reported values for gas ratios, though, are either absolute ratios, ‰ deviation from expected equilibrated value, or excess N_2 or O_2 concentration relative to the equilibrium concentration. Reported isotope values are in the delta notation relative to the atmospheric air standard (AIR). This AIR primary standard was provided and certified by Ralph Keeling (Scripps Institution of Oceanography, pers. comm.) permitting the absolute N_2/Ar and O_2/Ar values and $\delta^{15}N_2$ and $\delta^{18}O_2$ values of our day-to-day standards (namely N_2+Ar+O_2, N_2+Ar, and pure O_2) relative to atmosphere to be determined.

In the "with O_2 mode," O_2/Ar ratios are reported, and $\delta\ ^{18}O_2$ values are calculated using the N_2+Ar+O_2 (peak 1) as a standard. Alternatively, N_2+Ar and low O_2 mix (peak 2) can be used when samples of known low O_2 concentrations are analyzed. Theoretically, the O_2 content in this reference gas mix can be adjusted to suit different samples, thus minimizing the interference effect produced by varying sample O_2/N_2 (see the next section). In the "no O_2 mode," N_2/Ar ratios are reported and $\delta^{15}N_2$ values are calculated from using the N_2+Ar (peaks 4 and 6) as standards. Earlier on in our development, we used only one standard peak for this part of the analysis. However, we found that improved reproducibility of $\delta^{15}N_2$ could be achieved by having two references of N_2-Ar bracketing the sample gas. The averaging effect reduces drift in the isotopic values of the standard gas, resulting in better precision. The standard deviations for $\delta^{15}N_2$ for the same seawater samples decreased from 0.034‰ (n = 15, 1 reference injection) to 0.013‰ (n = 14, 2 reference injections).

Correction for varying O_2/N_2

Variations in sample O_2 content are well known to influence observed gas and isotopic ratios as a result of ion-ion interactions and trace formation of isobaric interferences in the IRMS ion source (e.g., Emerson et al. 1999; Bender et al. 1994). These effects are particular to each instrument and its ion source settings. The easiest solution for accurate measurement of N_2/Ar and $\delta^{15}N_2$ is O_2 removal as discussed above. For $\delta^{18}O_2$ determination, to achieve accurate results, a calibration and subsequent correction for the influence of changing O_2/N_2 must be made (Emerson et al. 1999; Quay et al. 1993).

Prior studies needed to laboriously pre-mix O_2 and N_2 in a series of flasks (Emerson et al. 1999). Here we use our custom reference gas system, in which the N_2+Ar reference gas and an O_2 reference gas can be introduced together. The O_2 content is quickly changed by altering the pressure on the O_2 capillary through a pressure control valve. This mixture is typically analyzed against the N_2+O_2+Ar reference and in practice calibrations for N_2/Ar and $\delta^{15}N_2$ are also obtained. This approach is also taken for accurate calibration of reference gases against the AIR standard.

We demonstrate here that such interference on $\delta^{15}N_2$ and $\delta^{18}O_2$ occurs in a linear fashion and can be easily corrected for. To assess the effect of O_2-N_2 interaction in the ion source, the N_2+Ar reference gas with varying amounts of pure O_2 is introduced in alternation with the N_2+Ar+O_2 reference gas. At the start of this experiment, the N_2 and O_2 of the former gas mixture is adjusted to the same level as the latter. Subsequently, the O_2 is reduced stepwise to 10 different O_2 concentrations until around 8-10% of its original level.

As shown in Fig. 4, strong relationships with varying sample O_2/N_2 ratios are observed for both $\delta^{15}N_2$ and $\delta^{18}O_2$. We observe a linear increase in the $\delta^{15}N_2$ values (Fig. 4A) with increasing O_2/N_2 ratios in the sample gas mixture allowing a straightforward correction to be applied to account for this variation. However as our routine $\delta^{15}N_2$ measurements for the samples utilize the O_2 removal scheme, these measurements are redundant. For $\delta^{18}O_2$, values increase as O_2/N_2 ratios increase or as N_2/O_2 ratios decrease (Fig. 4B). We assessed the effect of O_2-N_2 interaction by running this test every other month or every time the working reference gas tank is replaced. The slope of each plot in Fig. 4A and 4B are used as a correction factor to account for the effect of O_2-N_2 interaction. Throughout the 13 tests run over the period of 28 months, we found that the correction factors are relatively stable despite the reference gas tank replacements. The correction factors for $\delta^{15}N_2$ and $\delta^{18}O_2$ are 4.21 ± 0.02 and –8.19 ± 0.06, respectively (Fig. 4).

The influence of O_2-N_2 interaction has also been reported on the gas ratio signals (Emerson et al. 1999). Here, we test the effect of O_2 on the observed N_2/Ar ratios by introduction of N_2+Ar (as reference) and a mixture of N_2+Ar and varying pure O_2 (referred to as sample). Similar to the previous section, the amount of N_2 gas from both reference and sample is matched

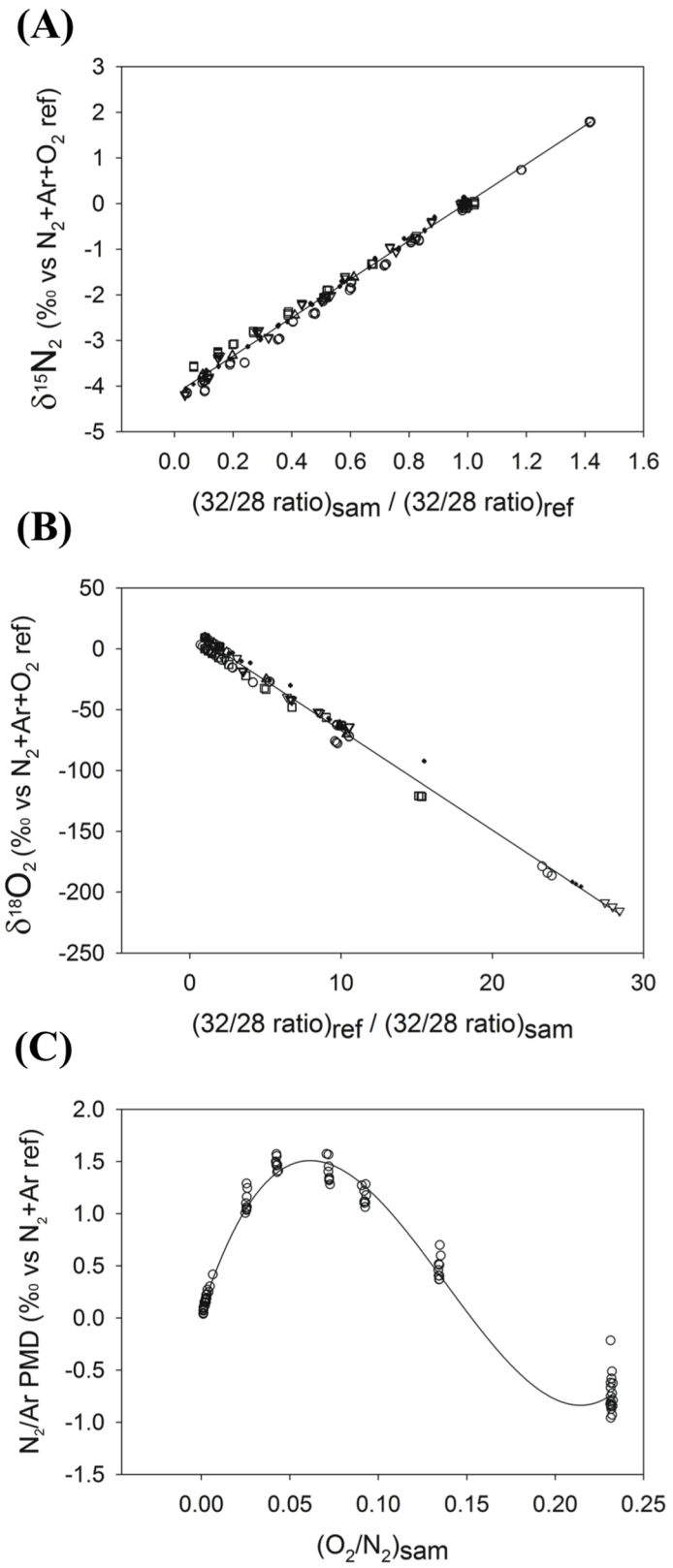

before the start of the test. Different amounts of O_2 are used (same level as described above) and the ‰ deviation in observed N_2/Ar relative to expected N_2/Ar are plotted (Fig. 4C). Our results show that the N_2/Ar ratios increase (deviating from the expected ratios) until the pivoting point where O_2/N_2 = 0.05 then the measured ratios start to drop steadily. While the overall range is ~2 ‰, there is clear influence of O_2/N_2 on the measured N_2/Ar ratios. While corrections can readily be made, in practice we use "no O_2" mode for the N_2/Ar ratio because of the lack of interference, and the variations in the measured N_2/Ar ratios from "with O_2" mode is generally greater than from those from "no O_2" mode. Where an O_2 removal system is not readily available, we recommend a careful calibration covering a large range of O_2/N_2 ratios to be expected from actual samples. Alternatively, using working standard gas with similar O_2/N_2 ratio to the samples can also help to remove the effect from this interference in the ion source.

Standardization and data treatment

Mass signal intensities are integrated for the flat top portions of the reference and sample peaks, respectively, with baseline intensity subtracted. Gas and isotope ratios are calculated using the 'δ' notation in ‰ units relative to the 2 working reference gases (wrg) as described above (Eq. 1). These are termed the raw δ-values. Each reference gas has been separately calibrated using the MC-IRMS against an AIR standard. In this regard, the true δ-values of the wrg (Eq. 2) are determined by alternating injections of the wrg with the AIR standard.

$$\delta_{true(wrg)} = \left[\left(\frac{R_{wrg}}{R_{AIR}}\right) - 1\right] \times 1000 \quad (2)$$

In principle, the raw δ-values of the samples can be used to calculate the "true" δ-values of the sample by using the following equation:

$$\delta_{true(sam)} = \delta_{raw(sam)} + \delta_{true(wrg)} + \left(\frac{\delta_{raw(sample)} \times \delta_{true(wrg)}}{1000}\right) \quad (3)$$

However, in some cases (i.e., measurements from "with O_2" mode including the O_2/Ar and $\delta^{18}O_2$), correction for varying O_2/N_2 must be made while day-to-day variations are also accounted for using the air-equilibrated seawater standards. Detailed data processing protocol is described below.

Fig. 4. Measurements of $\delta^{15}N_2$ and $\delta^{18}O_2$ with sample O_2/N_2 ratios relative to the reference, for the $\delta^{15}N_2$ plot (A), the corresponding value on this x-axis is 1 at 100% O_2 (i.e., samples have the same O_2 concentrations as the reference), and becomes smaller as O_2 level decreases. For $\delta^{18}O_2$ plot (B), however, the corresponding value on the x-axis becomes larger as the O_2 levels decrease. Both (A) and (B) are taken from 13 tests run over 28 months (indicated by different symbols). (C) The change in the N_2/Ar ratio as a function of O_2/N_2. The expected ratios of N_2/Ar are taken from the reference gas with no O_2 (N_2 + Ar) whereas the observed sample ratios are from the gas mixture of N_2 + Ar and pure O_2 (at varying amount) from 2 tests run over 3 months. Lines are derived from a least squares linear/polynomial fit to the data points. The slopes (±SE) for (A) $\delta^{15}N_2$ and (B) $\delta^{18}O_2$ are 4.21 ± 0.02 and –8.19 ± 0.06, respectively. Note: Horizontal axes differ in each panel.

For the calculation of excess N_2 (i.e., observed N_2 concentration above that expected at a specific temperature and salinity), we first take the raw delta N_2/Ar value of the sample ("no O_2" mode) versus the N_2-Ar working reference gas (from Eq. 1) and convert it to the observed sample ratio (Obs N_2/Ar).

$$Obs\ N_2 / Ar = \left(\frac{\delta_{raw(sam)}\ N_2 / Ar}{1000} + 1 \right) \times N_2 / Ar_{true(wrg)} \quad (4)$$

From the observed sample ratio, a ‰ deviation (PMD) with respect to the expected ratio is calculated. Expected ratios are calculated assuming equilibration with the atmosphere at observed in situ temperature and salinity, using solubility coefficients from Hamme and Emerson (2004) for Ar and N_2:

$$\text{PMD} = \left(\frac{Obs\ N_2 / Ar}{Equil\ N_2 / Ar} - 1 \right) \times 1000 \quad (5)$$

To account for day-to-day variation in the extraction procedure, we adjust the PMD using the air-equilibrated seawater standards that are run at regular intervals throughout the sample batch. It is assumed that these air-equilibrated SW standards have an N_2/Ar ratio equivalent to that derived from solubility coefficients (Hamme and Emerson 2004), and hence, the PMD of those SW standards should be zero. An average value of any observed PMD for the SW standards is used as a SW standard correction factor (SWCF), and this is applied to every sample during that run. SWCF are regularly observed to fall in the range of –3.3 to –6.3 for the N_2/Ar ratio.

$$Adjusted\ PMD = PMD + SWCF \quad (6)$$

This adjusted PMD (adj.PMD) can then be used to determine the excess N_2 concentration in μmol/kg.

$$Excess\ N_2 = \frac{adj.PMD}{1000} \times \left[Equil\ N_2 \right] \quad (7)$$

It should be noted that for studies assessing contributions from biogenic N_2, values are further corrected to subtract out the influence of background excess N_2, for example using waters outside oxygen deficient regions (Devol et al. 2006; Chang et al. 2010, 2012).

O_2/Ar is processed in an identical manner to provide excess O_2 values using solubility coefficients from García and Gordon (1992), and in turn, sample O_2 concentrations. O_2/Ar ratios are taken from the "with O_2" mode using the N_2-Ar-O_2 as the working reference gas. For both excess N_2 and O_2, this formulation assumes that Ar concentrations are at equilibrium values. Deviations from this have been observed in the ocean due to physical effects, such as bubble injection and subduction of a water mass without complete air-sea gas exchange in water mass formation regions (Emerson et al. 1995; Hamme and Emerson 2002). However, these deviations are only of the order of 2% (Hamme and Emerson 2002) and would produce corresponding errors in excess concentration.

As for $\delta^{15}N_2$, we first obtain the $\delta^{15}N_2$ of sample versus N_2-Ar wrg from the "no O_2" mode [$\delta_{15}N_{2\text{raw(sam)}}$], which we then use to determine $\delta^{15}N_2$ sample vs AIR [$\delta_{15}N_{2\text{true(sam)}}$]. We again use the SW standards to correct for day-to-day variation in an identical manner to the gas ratios (N_2/Ar and O_2/Ar).

$$Adjusted\ \delta^{15}N_2 = \delta^{15}N_{2\ true(sam)} + SWCF \quad (8)$$

Isotope anomalies are calculated by subtracting the observed δ values from those expected at equilibration with atmosphere at *in situ* temperature and salinity based on Klots and Benson (1963) for $\delta^{15}N_2$ and from Benson et al. (1979) for $\delta^{18}O_2$.

$$PMD = Observed\ \delta\ value - Expected\ \delta\ value \quad (9)$$

The $\delta^{18}O_2$ can be obtained in the same way as for $\delta^{15}N_2$ except that an additional correction factor is required for $\delta^{18}O_2$ to take into account interference in the ion source (see above). This is done based on the ion source correction factor (*ion_source_CF*) determined over varying O_2/N_2 (Fig. 4B). The following equation is substituted for Eq. 3, but then an identical procedure to $\delta^{15}N_2$ is followed to complete the data correction.

$$\delta^{18}O_{true(sam)} = \delta^{18}O_{raw(sam)} + ion_{source_{CF}} + \delta^{18}O_{true(wrg)} + \left(\frac{\delta_{raw(sample)} \times \delta_{true(wrg)}}{1000} \right) \quad (10)$$

The ion source correction factor (*ion_source_CF*) shown in Eq. 10 is derived from the linear relationship between observed $\delta^{18}O_2$ values over varying O_2/N_2 ratios (shown in Fig. 4B).

Assessment

Reference gas standards

The two wrg standards are tested daily for analytical reproducibility before any sample analyses as part of our quality control procedures. Nine injections of the reference gas to the IRMS are made, and the reported gas ratios or isotopic composition are assessed for their standard deviations. The precisions of standard gas replicates were better than 0.3‰ for gas ratios and 0.04‰ for isotope ratios (Table 1). These values are directly comparable with those for standard gas replicates by the EQ benchmark method (Table 1).

Air-equilibrated seawater

To assess precision and accuracy of our dissolved gas extraction and purification procedures, a series of air-equilibrated seawater standards were analyzed and compared to theoretical values over a range of temperatures. One-liter glass flasks containing seawater were placed in high precision water baths (as stated above) set at specified temperatures (t = 5°C, 10°C, 15°C, 20°C, 25°C, or 30°C) and gently stirred overnight to allow full equilibration with air. For each analytical run, the water standards at 15°C were used as an anchoring tempera-

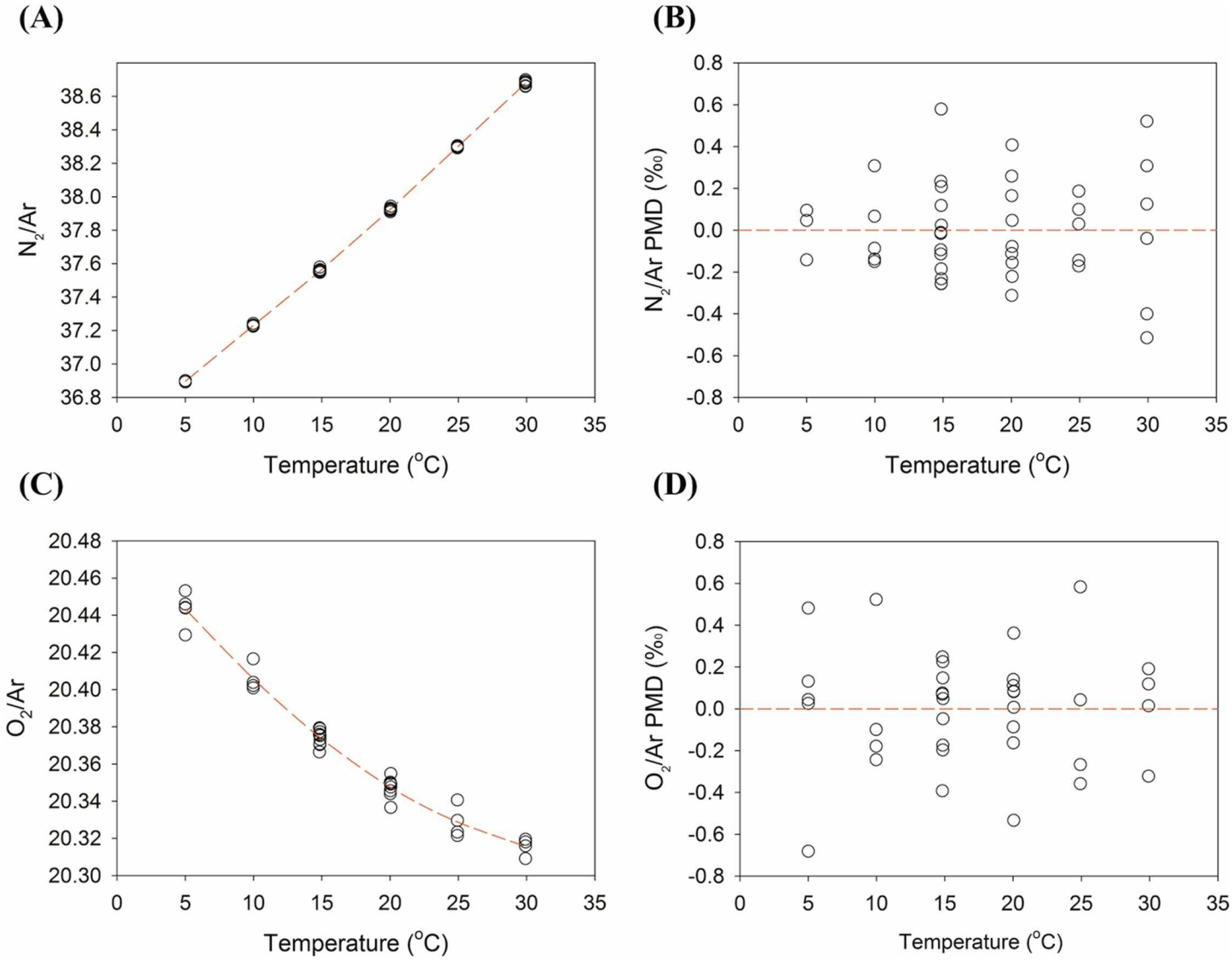

Fig. 5. The gas ratios of air equilibrated seawater standards. The N_2/Ar (A) and O_2/N_2 (C) ratios as a function of temperature and the ‰ deviation from the expected ratios for the N_2/Ar (B) and O_2/N_2 (D) ratios are shown here. The red dotted lines represent the expected ratios (based on equations from Hamme and Emerson [2004] for N_2 and Ar and García and Gordon [1992] for O_2). Note: Per mil deviation (PMD) is calculated using Eq. 5 (see text).

ture to account for any day-to-day drift in system response. Similar to the application of a SWCF described above for sample analysis in the previous section, a minor correction factor was derived from the difference between the expected ratio and the mean of raw observed ratios only for the 15°C water standard. This SWCF was applied to every analysis made for the other water standards throughout the day. The salinity of each standard was also carefully checked as small changes might have occurred due to evaporation, and adjustments were made as needed to account for this small variation in salinity.

Plotting the adjusted observed ratios for N_2/Ar and O_2/Ar against the temperature at which the standards were equilibrated (Fig. 5A and 5C) shows that the observed data points are located very close to the line of expected equilibrium values (on average 0.02% difference for both ratios). To further illustrate how well these data compare, we determine the PMD from the expected ratios (Fig. 5B and 5D), which more clearly demonstrates how close the data points are to the expected values (i.e., located along the 0‰ line). There is no systematic bias and the PMD ranges between 0.14‰ and 0.57‰ for N_2/Ar ratios and between 0.32‰ and 0.68‰ for O_2/Ar ratios. The mean ‰ standard deviations calculated from these measurements were 0.23‰ and 0.53‰ for N_2/Ar and O_2/Ar, respectively, which is close to the precision of standard gas replicates (Table 1).

The plots of isotopic compositions as a function of temperature and their deviations from the expected values are shown

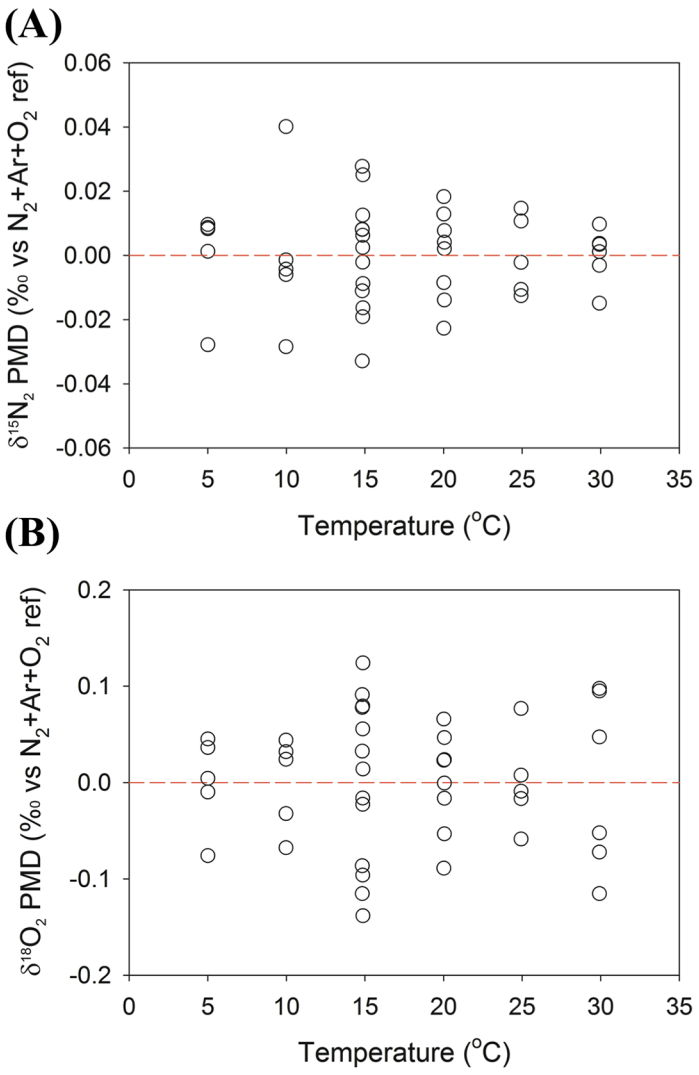

Fig. 6. The PMD of air equilibrated water standards from the expected values (based on equations from Klots and Benson [1963] for $\delta^{15}N_2$ and Benson et al. [1979] for $\delta^{18}O_2$; dotted lines) for (A) $\delta^{15}N_2$ and (B) $\delta^{18}O_2$.

in Fig. 6. A similar anchoring scheme using 15°C water was carried out and the PMD plotted. Similar to the gas ratios, our adjusted observed measurements show consistency with the expected isotopic values without any systematic bias. The PMD ranges between 0.01 and 0.04 for $\delta^{15}N_2$ and between 0.07 and 0.14 for $\delta^{18}O_2$. The average values for the standard deviations (as shown in Table 1) are 0.02‰ and 0.09‰ for $\delta^{15}N_2$ and $\delta^{18}O_2$, respectively; again as for the gas ratios, these values agree well with those for the standard gas replicates (Table 1).

Performance for field-collected samples

Field samples were collected from the Bermuda Atlantic Time-series Study (BATS) station located at 31°40′N 64°10′W. In August 2012, triplicate samples from 24 depths were collected from the surface water down to 1000 m following the protocol outlined above. Concurrently, physical parameters including temperature and salinity (using SBE-911plus sensor) and dissolved oxygen (SBE-43 sensor) were also measured. The depth profiles for excess N_2 concentration, $\delta^{15}N_2$ anomaly, O_2 concentration, $\delta^{18}O_2$ anomaly are shown in Fig. 7 to illustrate the use of this method in the field. The excess N_2 profile (Fig. 7A) shows surface water having N_2 concentrations close to saturation (i.e., the excess N_2 being –0.07 μmol/kg). However, excess N_2 gets progressively larger until it reaches 3 μmol/kg at 150 m. From this depth down to 500 m, the excess N_2 does not show any appreciable changes. Below which, a noticeable increase in excess N_2 is observed with an excess of 7 μmol/kg seen at 1000 m depth. This increase in excess N_2 at depth can be explained by bubble injection when the water mass was formed at the surface. This process preferentially affects less soluble gases, such as N_2 compared with its more soluble counterparts (e.g., Ar), causing the N_2/Ar ratio to be larger than that expected from gas solubility alone (Emerson et al. 1991). The standard deviations of triplicate samples over the depth range sampled ranged from 0.002 to 0.78 μmol/kg, with a mean of 0.32 μmol/kg. This corresponds to a relative standard deviation value of 0.39‰. The average difference between paired samples of 0.59‰ agrees well with that observed using the EQ benchmark (0.6‰; Table 1).

The anomalies of $\delta^{15}N_2$ (i.e., the deviation from the expected $\delta^{15}N_2$ values at a specified temperature) are plotted in Fig. 7B. Slightly enriched $\delta^{15}N_2$ values are observed above 30 m, whereas all sample below that are isotopically depleted. The average difference between paired samples is 0.02‰ (reported in Table 1) with the range from 0.001 to 0.048‰. This level of precision is comparable with that of the EQ benchmark (0.03‰; Table 1). To evaluate the increased precision in $\delta^{15}N_2$ measurements provided by the "no O_2" mode, we compared $\delta^{15}N_2$ values from the same depth profile between the two oxygen modes (Fig. 8). Noticeably larger standard deviations are inherent of data from the "with O_2" mode while clearly oxygen removal helps to diminish the spread of the data. Also, more importantly, the values from the "with O_2" mode are overestimated by as much as 1.57 ‰ when compared with their "no O_2" counterparts (Fig. 8). Note that the data from the "with O_2" mode have been corrected for O_2-N_2 interactions. However, this correction does not account for any interference at mass 29 (i.e., $^{15}N^{14}N$) by the production of $^{13}C^{16}O$ (Bender et al. 1994) potentially caused by the introduction of CO_2 or the interaction between any hydrocarbons (CH_x) and O_2 within the ion source. An additional liquid nitrogen trap to remove CO_2 and a VOC trap to remove CH_x might be another solution to this problem. We found that these interferences can be easily eliminated by our O_2 removal system, which simultaneously removes O_2, CO_2, and CH_x from the sample gas. Therefore, it appears that not only can we achieve higher precisions for $\delta^{15}N_2$ measurements through the use of an O_2 removal subsystem, the overestimation of reported values can also be avoided. In contrast to a recent approach (Fuchsman et al. 2008), we posit that O_2 removal is required for both precise and accurate $\delta^{15}N_2$ measurements.

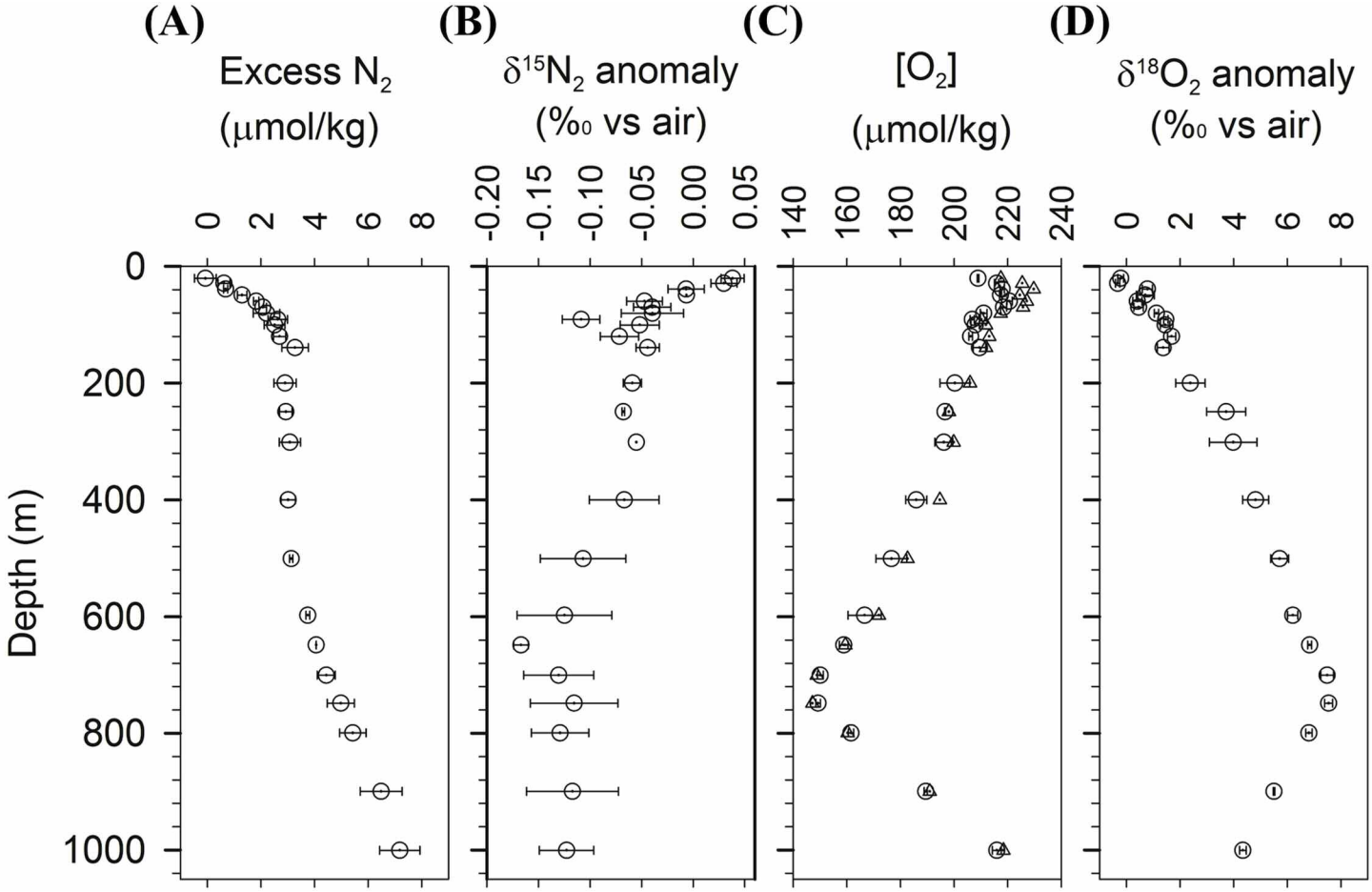

Fig. 7. Depth profiles of (A) excess N_2, (B) $\delta^{15}N_2$ anomaly, (C) O_2, and (D) $\delta^{18}O_2$ anomaly at BATS (July 2012). The triangles in (C) are data from Winkler-calibrated SBE-43 sensor. Error bars represent one standard deviation for each set of triplicate samples.

Depth profiles of O_2 (Fig. 7C) were used to evaluate the accuracy of O_2 concentrations determined from the IRMS versus those obtained from the SBE43 sensor (calibrated with Winkler titrations). To assess accuracy, the percentage difference between IRMS-derived values and their counterparts were calculated. The average % difference between the two methods to determine O_2 concentration was only 2%, thereby providing confidence in our measurements. As for precision, we observed standard deviations for triplicate samples ranging from 0.18 to 6.19 μmol/kg, with an average of 1.86 μmol/kg.

Lastly, the $\delta^{18}O_2$ anomalies (i.e., the deviation from the expected $\delta^{18}O_2$ values at a specified temperature) are plotted in Fig. 7D. This depth profile is virtually an inverse of the O_2 concentrations; $\delta^{18}O_2$ becomes more enriched as O_2 concentrations diminish, and vice versa. This is a result of the isotope effect associated with water column respiration (Kroopnick and Craig 1976). Our precisions for the $\delta^{18}O_2$ measurements were on average 0.24‰ (standard deviations ranging from 0.028‰ to 0.88‰). The average difference between paired samples observed for these samples was 0.22‰, which is marginally greater than the value reported for the EQ benchmark (0.04‰; Table 1).

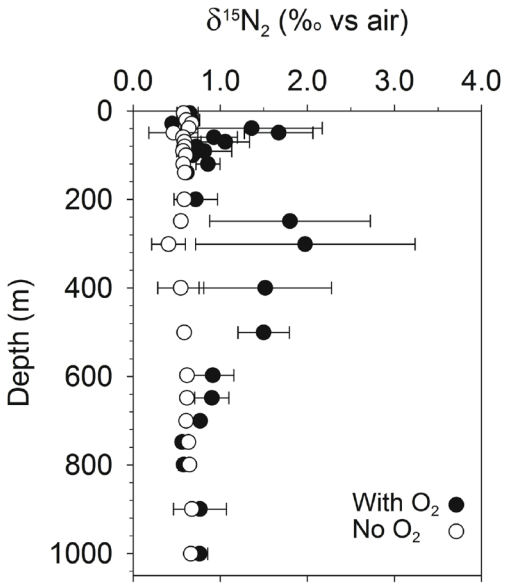

Fig. 8. The comparison of the $\delta^{15}N_2$ measurements between the "no O_2" and "with O_2" modes.

Table 2. Longevity of collected samples.

Time	Excess N_2 (μmol/kg)	Excess O_2 (μmol/kg)
Initial (n = 5)	74.45 ± 0.87	–237.6 ± 3.39
1 week (n = 4)	75.33 ± 0.47	–230.7 ± 2.83*; P = 0.01
2 weeks (n = 4)	75.46 ± 0.52	–227.6 ± 1.02*; P = 0.00
4 weeks (n = 4)	76.16 ± 0.65	–228.3 ± 2.24*; P = 0.00
10 weeks (n = 4)	77.39 ± 1.02	–226.5 ± 4.60*; P = 0.00
4 months (n = 4)	76.57 ± 1.00	–214.8 ± 6.03*; P = 0.00
6 months (n = 4)	75.01 ± 1.06	–201.1 ± 2.69*; P = 0.00

Values reported are average ± 1 SD of gas concentrations in μmol/kg. Asterisks indicate values that are significantly different from those of the initial time point with reported P values (from Student t test).

Sample longevity

In practice, many months may pass between sample collection and laboratory analysis. A test of the stability of $HgCl_2$ preserved samples was carried out in order to determine allowable storage times for N_2 and O_2. Filtered seawater in a 20-L carboy was bubbled overnight with N_2-Ar gas in a temperature controlled room (10°C). About 15 min before sampling, bubbling was stopped while gentle stirring kept the seawater well-mixed. Water was filled into 60-mL glass bottles, following the protocol outlined above. Samples for the initial time point were analyzed on the same day as collection, with subsequent time points analyzed afterwards at 1-week, 2-week, 4-week, 10-week, 4-month, and 6-month intervals (Table 2; n = 4 for all time points, except T_0 where n = 5). The excess N_2 values in samples stored for up to 6 months (6 mo = 75.01 μM ± 1.06 μM) were not significantly different from the T_0 samples (T_0 = 74.45 μM ± 0.87 μM) of the experiment ($P > 0.05$). In contrast, significant differences were observed for excess O_2 values in all the stored samples, with the difference increasing with time. After six months, the excess O_2 value was 35 μM (c.a. 15%) higher than at the initial time point.

These observations suggest that samples are able to be stored for long periods of time (up to 6 months) while not sacrificing the integrity for N_2 concentrations. The O_2 results suggest some exchange with the atmosphere over time using these materials, whether this is only significant under low oxygen conditions as simulated in this test remains to be determined. While it is best to analyze samples as soon as possible, these results suggest that it may be possible to develop a correction for storage time.

Discussion

Our method's precisions are comparable with Emerson et al. (1991) for both gas ratios and isotopic compositions as indicated in Table 1. These levels of precision cannot be achieved by the MIMS measurements, which are worse by approximately an order of magnitude (7‰ for N_2/Ar and 19‰ for O_2/Ar as reported in Tortell 2005). In addition to having achieved equally high precisions to the EQ benchmark, our method also has several distinct advantages. One of which is the ease of sampling. As discussed earlier, a goal during method development was to produce a simple sample collection procedure that enabled rapid filling of bottles allowing more samples to be collected without compromising the integrity. Our off-the-shelf 60-mL serum bottles are considerably less expensive and smaller than the evacuated 250-mL glass flasks typically used for sampling for the EQ benchmark method, allowing for more bottles to be brought on board during sampling cruises. Additionally, we do not need additional sampling apparatus such as a CO_2 tank required for bottle flushing as described in the EQ method; such additional steps further limit the numbers of samples to be collected on each cruise. Using our simple sampling protocol with smaller sample bottles, we have successfully collected over 1500 samples during a 1-month long cruise, resulting in a much larger dataset of excess N_2 and $\delta^{15}N_2$ in the eastern equatorial Pacific and the oxygen deficient zone (ODZ) of the Eastern Tropical South Pacific (ETSP). Chang et al. (2010) reported gas profiles from 2 stations within the ETSP ODZ whereas our current method has allowed more than 40 stations to be sampled. In fact, the sampling procedure described in this study is simple enough to allow one person to typically finish triplicate sampling from one Niskin bottle within 5 minutes. Moreover, our serum bottles (c.a. $2 each) are much less costly than the bottles used in the EQ benchmark method (c.a. $80 each; B.X. Chang, pers. comm.), making it much more affordable without any compromise in precision or accuracy. Furthermore, the EQ benchmark approach uses larger and more expensive sampling bottles and a more complicated sampling procedure which both greatly constrain the number of samples that can be collected at sea.

Shorter analysis time is another major advantage of our method. As opposed to the EQ benchmark where long equilibration at controlled temperature (4 h) is required, we use an on-line whole-water gas extraction where all dissolved gases are stripped from the water phase by the He carrier gas and transported into the preparation system. The typical analysis time for our method is under 8 min per one sample, enabling the average throughput of 50 samples per day. In contrast, the EQ benchmark is typically capable of analyzing c.a. 10 samples per day (B.X. Chang, pers comm). This can be achieved without compromising the precision of the reported values. Hence, we are able to achieve much higher sample throughput as compared with the EQ benchmark. However, we can achieve very high precisions comparable to the EQ benchmark, and we are also able to measure the isotopic compositions of the dissolved gases simultaneously, which cannot be achieved with a MIMS.

High precisions for both $\delta^{15}N_2$ and $\delta^{18}O_2$ achieved through the use of this present method allow application of isotopic signals at natural abundance levels to efficiently trace different oceanic processes including primary production, respiration (through the use of ^{18}O), and denitrification (through

^{15}N). Notably with the enhanced precision for $\delta^{15}N_2$ attained with bracketing the sample peak with two reference peaks during the no-O_2 mode of the analysis, any changes as small as 0.02‰ in the $\delta^{15}N_2$ can be determined. We have applied this to the samples collected from the Peru ODZ collected in 2012, which show unprecedented highly resolved changes in the $\delta^{15}N_2$ produced by N-loss processes (manuscript in prep).

Comments and recommendations

Although it is highly advisable that the samples collected be analyzed as soon as possible (at best within 2 weeks of collection), we are currently exploring different modifications to lengthen the storage time. While the butyl stoppers remain the most favorable choice due to ease of sampling, their pretreatment such as degassing with He (De Brabandere et al. 2012) prior to being used for sampling might help to remove any trace gases present in the stopper, which can alter the content of the dissolved gas sample during storage. This might be particularly useful in the case where a gas of interest is scarce (e.g., low O_2 content in the OMZs).

Alternative preservatives for sample preservation are also being explored. In some cases, adding $HgCl_2$ to the serum bottle during sampling is not permitted near the rosette or poses hazardous materials issues for subsequent handling and shipping. Consequently, the samples have to be "killed" at a later time requiring piercing the stopper with a needle. This is not an optimal technique as punctures might lead to leakage of sample or air bubbles might be introduced to the samples. To circumvent this problem, we have recently found that HCl and formalin can be substituted as a preservative as it does not interfere with our analytical procedure.

More extensive preservation tests are underway to better determine storage time for the different types of dissolved gas samples (e.g., oxic and anoxic seawater) and for the different types of preservatives (e.g., HCl and formalin). As the test described earlier in this article simulated the condition in an OMZ (high N_2 and low O_2), samples collected under fully oxic conditions might behave differently during storage. This additional test will pinpoint if O_2 has a shorter storage time similar to what we found in the test conducted in this study. One measurement that our method has the potential to evaluate is $\delta^{17}O_2$. Precise measurements of the natural abundance of stable oxygen isotopes (^{16}O, ^{17}O, ^{18}O) in dissolved oxygen (triple oxygen isotopes) can be used to assess gross primary production (Nicholson et al. 2012; Luz and Barkan 2000; Luz et al. 1999). Our method has not yet attained high enough precision to be used for that purpose, but this is one of the potential areas for further development.

References

Bange, H. W., S. Rapsomanikis, and M. O. Andreae. 2001. Nitrous oxide cycling in the Arabian Sea. J. Geophys. Res. Oceans 106(C1):1053-1065.

Bender, M. L., and K. D. Grande. 1987. Production, respiration, and the isotope geochemistry of O_2 in the upper water column. Global Biogeochem. Cycl. 1(1):49-59 [doi:10.1029/GB001i001p00049].

———, P. P. Tans, J. T. Ellis, J. Orchardo, and K. Habfast. 1994. A high-precision isotope ratio mass-spectrometry method for measuring the O_2:N_2 ratio of air. Geochim. Cosmochim. Acta. 58(21):4751-4758 [doi:10.1016/0016-7037(94)90205-4].

Benson, B. B., D. Krause Jr, and M. A. Peterson. 1979. The solubility and isotopic fractionation of gases in dilute aqueous solution. I. Oxygen. J. Solut. Chem. 8(9):655-690 [doi:10.1007/BF01033696].

Cassar, N., B. A. Barnett, M. L. Bender, J. Kaiser, R. C. Hamme, and B. Tilbrook. 2009. Continuous high-frequency dissolved O_2/Ar measurements by equilibrator inlet mass spectrometry. Anal. Chem. 81(5):1855-1864 [doi:10.1021/ac802300u].

Chang, B. X., A. H. Devol, and S. R. Emerson. 2010. Denitrification and the nitrogen gas excess in the eastern tropical South Pacific oxygen deficient zone. Deep Sea Res. I 57(9):1092-1101 [doi:10.1016/j.dsr.2010.05.009].

———, ———, and ———. 2012. Fixed nitrogen loss from the eastern tropical North Pacific and Arabian Sea oxygen deficient zones determined from measurements of N_2:Ar. Global Biogeochem. Cycl. 26(3) [doi:10.1029/2011GB004207].

De Brabandere, L., B. Thamdrup, N. P. Revsbech, and R. Foadi. 2012. A critical assessment of the occurrence and extend of oxygen contamination during anaerobic incubations utilizing commercially available vials. J. Microbiol. Methods 88(1):147-154 [doi:10.1016/j.mimet.2011.11.001].

Devol, A. H., and others. 2006. Denitrification rates and excess nitrogen gas concentrations in the Arabian Sea oxygen deficient zone. Deep Sea Res. I 53(9):1533-1547 [doi:10.1016/j.dsr.2006.07.005].

Emerson, S., P. Quay, C. Stump, D. Wilbur, and M. Knox. 1991. O_2, Ar, N_2, and ^{222}Rn in surface waters of the subarctic ocean: Net biological O_2 production. Global Biogeochem. Cycl. 5(1):49-69 [doi:10.1029/90GB02656].

———, ———, ———, ———, and R. Schudlich. 1995. Chemical tracers of productivity and respiration in the subtropical Pacific Ocean. J. Geophys. Res. 100(C8):15873-15887 [doi:10.1029/95JC01333].

———, C. Stump, D. Wilbur, and P. Quay. 1999. Accurate measurement of O_2, N_2, and Ar gases in water and the solubility of N_2. Mar. Chem. 64(4):337-347 [doi:10.1016/S0304-4203(98)00090-5].

Fuchsman, C. A., J. W. Murray, and S. K. Konovalov. 2008. Concentration and natural stable isotope profiles of nitrogen species in the Black Sea. Mar. Chem. 111(1-2):90-105 [doi:10.1016/j.marchem.2008.04.009].

Gaarder, T., & Gran, H. H. (1927). Investigations of the production of plankton in the Oslo Fjord. Conseil permanent international pour l'exploration de la mer.

García, H. E., and L. I. Gordon. 1992. Oxygen solubility in seawater—Better fitting equations. Limnol. Oceanogr. 37(6):1307-1312 [doi:10.4319/lo.1992.37.6.1307].

Hamme, R. C., and S. R. Emerson. 2002. Mechanisms controlling the global oceanic distribution of the inert gases argon, nitrogen and neon. Geophys. Res. Lett. 29(23):2120 [doi:10.1029/2002GL015273].

———, and ———. 2004. The solubility of neon, nitrogen and argon in distilled water and seawater. Deep Sea Res. I 51(11):1517-1528 [doi:10.1016/j.dsr.2004.06.009].

Luz, B., E. Barkan, M. L. Bender, M. H. Thiemens, and K. A. Boering. 1999. Triple-isotope composition of atmospheric oxygen as a tracer of biosphere productivity. Nature. 400(6744):547-550 [doi:10.1038/22987].

——— and ———. 2000. Assessment of oceanic productivity with the triple-isotope composition of dissolved oxygen. Science. 288(5473):2028-2031 [doi:10.1126/science.288.5473.2028].

Kana, T. M., C. Darkangelo, M. D. Hunt, J. B. Oldham, G. E. Bennett, and J. C. Cornwell. 1994. Membrane inlet mass spectrometer for rapid high-precision determination of N_2, O_2, and Ar in environmental water samples. Anal. Chem. 66(23):4166-4170 [doi:10.1021/ac00095a009].

———, M. B. Sullivan, J. C. Cornwell, and K. M. Groszkowski. 1998. Denitrification in estuarine sediments determined by membrane inlet mass spectrometry. Limnol. Oceanogr. 43(2):334-339 [doi:10.4319/lo.1998.43.2.0334].

Klots, C. E., and B. B. Benson. 1963. Isotope effect in the solution of oxygen and nitrogen in distilled water. J. Chem. Phys. 38(4):890 [doi:10.1063/1.1733778].

Kroopnick, P., and H. Craig. 1976. Oxygen isotope fractionation in dissolved oxygen in the deep sea. Earth Planet. Sci. Lett. 32(2):375-388 [doi:10.1016/0012-821X(76)90078-9].

Nicholson, D. P., R. H. R. Stanley, E. Barkan, D. M. Karl, B. Luz, P. D. Quay, and S. C. Doney. 2012. Evaluating triple oxygen isotope estimates of gross primary production at the Hawaii Ocean Time–series and Bermuda Atlantic Time–series Study sites. J. Geophys. Res. Oceans. 117, C05012 [doi:10.1029/2010JC006856].

Quay, P. D., S. Emerson, D. O. Wilbur, C. Stump, and M. Knox. 1993. The $\delta^{18}O$ of dissolved O_2 in the surface waters of the subarctic Pacific: a tracer of biological productivity. J. Geophys. Res. Oceans 98(C5):8447-8458.

———, C. Peacock, K. Björkman, and D. M. Karl. 2010. Measuring primary production rates in the ocean: Enigmatic results between incubation and non-incubation methods at Station ALOHA. Global Biogeochem. Cycl. 24(3) [doi:10.1029/2009GB003665].

Tortell, P. D. 2005. Dissolved gas measurements in oceanic waters made by membrane inlet mass spectrometry. Limnol. Oceanogr. Methods 3:24-37. Limnol. Oceanogr. Methods 3:24-37 [doi:10.4319/lom.2005.3.24].

Walter, S., H. W. Bange, U. Breitenbach, and D. W. Wallace. 2006. Nitrous oxide in the North Atlantic Ocean. Biogeosciences 3(4):607-619 [doi:10.5194/bg-3-607-2006].

Ward, B. B., and O. C. Zafiriou. 1988. Nitrification and nitric oxide in the oxygen minimum of the eastern tropical North Pacific. Deep Sea Res. A. 35(7):1127-1142 [doi:10.1016/0198-0149(88)90005-2].

Submitted 7 October 2013
Revised 28 February 2014
Accepted 11 Apri 2014